DOI https: //doi. org/10.1007/s11595-018-1845-4

Effects of Strain Rate and Texture on the Tensile Behavior of Pre-strained NiCr Microwires

ZHOU Xiuwen[1,2], QI Yidong[1,3], LIU Xudong[1], NIU Gao[1], YANG Bo[1], YANG Yi[1], ZHU Ye[1], YU Bin[1], WU Weidong[1,2]*

(1. Research Center of Laser Fusion, China Academy of Engineering Physics, Mianyang 621900,China; 2. Institute of Atomic and Molecular Physics, Sichuan University, Chengdu 610065, China; 3.State Key Laboratory Cultivation Base for Nonmetal Composites and Functional Materials, Southwest University of Science and Technology, Mianyang 621010, China)

Abstract: The stress–strain behavior and strain rate sensitivity of pre-strained Ni80Cr20 (Ni20Cr) were studied at strain rates from 4.8×10^{-4} s^{-1} to 1.1×10^{-1} s^{-1}. Specimens were prepared through cold drawing with abnormal plastic deformation. The texture of the specimen was characterized using electron backscatter diffraction. Results revealed that the ultimate tensile strength and ductility of the pre-strained Ni20Cr microwires simultaneously increased with increasing strain rate. Twinning-induced negative strain rate sensitivity was discovered. Positive strain rate sensitivity was present in fracture flow stress, whereas negative strain rate sensitivity was detected in flow stress values of $\sigma_{0.5\%}$ and $\sigma_{1\%}$. Tensile test of the pre-strained Ni20Cr showed that twinning deformation predominated, whereas dislocation slip deformation dominated when twinning deformation reached saturation. The trends observed in the fractions of 2°-5°, 5°-15°, and 15°-180° grain boundaries confirmed that twinning deformation dominated the first stage.

Key words: tensile behavior; strain rate sensitivity; Ni20Cr; microstructure characterization; microwire

1 Introduction

Production of bonding wires faces new challenges with the development of integrated circuit (IC) technology[1]. In addition, wire diameter must be decreased to meet the requirements of Z-pinch experiments and freezing engineering[2-6]. Cold drawing is an effective technology used to decrease wire diameter through either a single- or multiple-step process. Pre-strain occurs from the first to the second pass and then continuously increases in consecutive passes. After reduction of wire diameter, grain size reaches the nanometer scale. Nanostructures materials (ns) exhibit grain sizes smaller than 100 nm[7], whereas ultrafine crystalline materials demonstrate grain sizes between 100 μm and 1 μm[8,9]. Fabrication of ultra-fine wires requires an understanding of the plastic behavior of metals because ductility is important in cold drawing.

In polycrystalline materials, orientation and size of individual grain play an important role in deformation[10,11]. External factors also affect the plastic deformation mechanisms, such as strain rate[12-16], temperature[17-20], and forming technology. Numerous studies provide insights into the underlying mechanisms of plastic deformation. Researches also show that the tensile strength and ductility of metals can be improved by increasing strain rate[16,21-23]. Ductility enhancement at high strain rates could be attributed to high work-hardening rate. However, cryomilled ns 5083 Al alloy and ball-milled Cu exhibit an opposite behavior (*i e*, high ductility at low strain rates)[14]. This effect could be due to the diffusion-mediated stress relaxation[15].

Changes in strain rate are used to reveal the deformation mechanisms, but experimental data on strain rate sensitivity are insufficient. As such, further studies must be performed to elucidate possible relationships between the stress-strain behavior and the texture during plastic deformation because deformation texture depends on the active deformation modes. Moreover, systematic experimental data of strain rate dependence of tensile properties for different materials have yet to be obtained. Furthermore, the effect of strain rate on the tensile behavior of pre-strain materials must be determined for multi-pass cold drawing.

(Received: Mar. 7, 2017; Accepted: Apr. 12, 2017)

ZHOU Xiuwen(周秀文): Assoc. Res.; Ph D; E-mail: xiuwenzhou@caep.cn

*Corresponding author: WU Weidong (吴卫东):Prof.; Ph D; E-mail: wuweidongding@163.com

Funded by the National Natural Science Foundation of China (No. 11135007)

This paper aims to determine the effects of strain and texture on the strain rate sensitivity (SRS) in pre-strained Ni80Cr20 (Ni20Cr) microwires through tensile tests at room temperature. Results showed that grains are inefficient for dislocation storage and strain hardening and similar to coarse grain subjected to heavy cold work, such as equal channel angular pressing. The fabricated microwires are susceptible to plastic instabilities, such as necking in tension.

2 Experimental

This study used Ni20Cr microwires with face-centered cubic structure (fcc) and a chemical composition of Ni-20.037%Cr-1.037%Si-0.194%Mn-0.141%Fe-0.101%Ti-0.087%Al-0.023%Cu (wt%). Specimens were prepared through cold drawing from as-received microwires with diameter of 25.6 μm via one pass. Engineering strains were about 8.8%, 17.3%, 26.4%, 36.1%, and 46.6%, respectively.

Table 1 Strain rate parameters of tensile test

Tensile velocity/(mm/min)	Gauge length/mm	Strain rate/s^{-1}
1.3	*197	1.1×10^{-4}
1.3	45	4.8×10^{-4}
1.3	20	1.1×10^{-3}
13	20	1.1×10^{-2}
*130	20	1.1×10^{-1}
100	20	0.83×10^{-1}

*: The maximum of gauge length and tensile velocity are 50 mm and 100 mm/min in our testing machine, respectively. So gauge length and tensile velocity of 45 mm and 100 mm/min were adopted

The pre-strain specimens were deformed at strain rates of 4.8×10^{-4}, 1.1×10^{-3}, 1.1×10^{-2}, and 0.83×10^{-1} s^{-1} through tensile tests at room temperature, and the parameters are shown in Table 1. Both ends of the tensile specimen were held tightly by a clamp using a screw to adjust the degree of tightness in wedge-type grips attached to the upper and lower pull rods of the machine. During the deformation, fracture positions frequently occurred near the clamp. By adjusting the degree of tightness, data of fracture positions as the central section of the specimen were selected. At least five microwires of the same specimen were tested under each condition, and the average value was determined from each set of experimental data.

3 Results and discussion

3.1 Effects of tensile behavior and strain rate on ductility

Fig.1 illustrates the stress-strain curves of pre-strained Ni20Cr microwires tested at various strain rates. All results had not exonerated several existing extrinsic factors, such as residual stress, surface state, texture, and so on. Fig.1(a) demonstrates that the trends of stress-strain curves with different pre-strains were divided into five groups. Ultimate tensile strength (UTS) remarkably increased, whereas ductility decreased with increasing pre-strain. Each group contained four stress-strain curves at different strain rates. Work-hardening behavior and ductility evidently differed among various strain rates. Fig.1(b) shows that UTS exhibited a linear trend up to the pre-strain. The UTS of different pre-strains increased from 809 MPa to 1 192 MPa at the strain rate of 4.8×10^{-4} s^{-1}. When the strain rate increased to 0.83×10^{-1} s^{-1}, the UTS of different pre-strains increased from 854 to 1 205 MPa. Under the same strain rate and different pre-strain conditions, the UTS increments are approximately 383 MPa and 351 MPa respectively. As well as under the same pre-strain and different strain rate conditions, the UTS increments are approximately 30 to 48 MPa. Comparison of these results reveals that the effect of pre-strain on the UTS

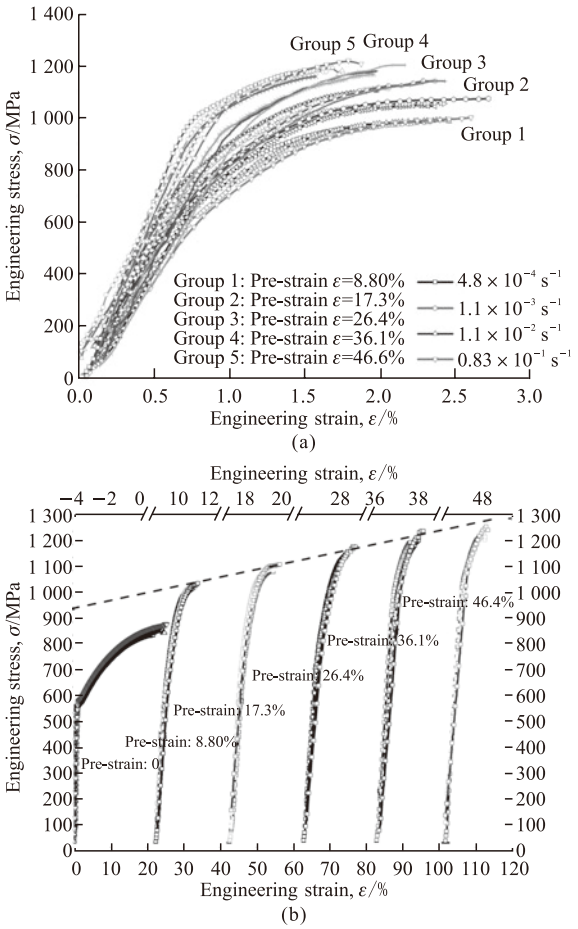

Fig.1 Stress-strain curves for pre-strains Ni20Cr microwires

is greater than the impact of strain rate. A similar trend was reported in the Refs.[24,25].

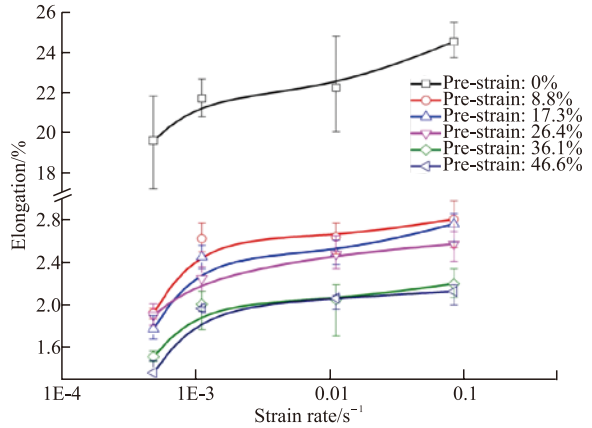

Fig.2 Elongation versus strain rate for pre-strains Ni20Cr microwires

The high strength of the specimen may be attributed to factors such as cellular refinement as a function of plastic strain, dislocation-line tension, and geometry of dislocation glide[26]. The dependence of strengthening on cellular refinement may be affected by the linear intercept between cell walls on the transverse section. Grain size strengthening follows the Hall-Petch effect, which is a linear law. The increment of elastic modulus was also considered because of the deformation texture behavior. The [001] texture increased the elastic modulus, which can be predicted using texture information[10].

Variations in fracture strain in the pre-strained Ni20Cr specimen were plotted as a function of strain rate as shown in Fig.2. The ductility of the Ni20Cr specimen increased at high strain rates. The strain rate dependence of fracture strain in the pre-strain specimen demonstrated a nonlinear increasing trend, especially at low rates. The phenomenon in the as-received specimen is similar to that in the pre-strained specimen. However, the enhanced ductility is a real abnormal phenomenon in different pre-strained specimens and significantly contributed to the deformation history. The fracture strains increased when strain rates increased from 4.8×10^{-4} s^{-1} to 1.1×10^{-3} s^{-1} in all pre-strained specimens and then increased slowly when strain rates increased from 1.1×10^{-3} s^{-1} to 0.83×10^{-1} s^{-1}.

The strain rate dependence of ductility shows similar strain rate dependence as in the ns Cu[24]. But it differs from that observed in ball-milled Cu[27] and cryomilled ns 5 083 Al alloy[14], in which fracture strain slightly decreases at high strain rates. Molecular dy-

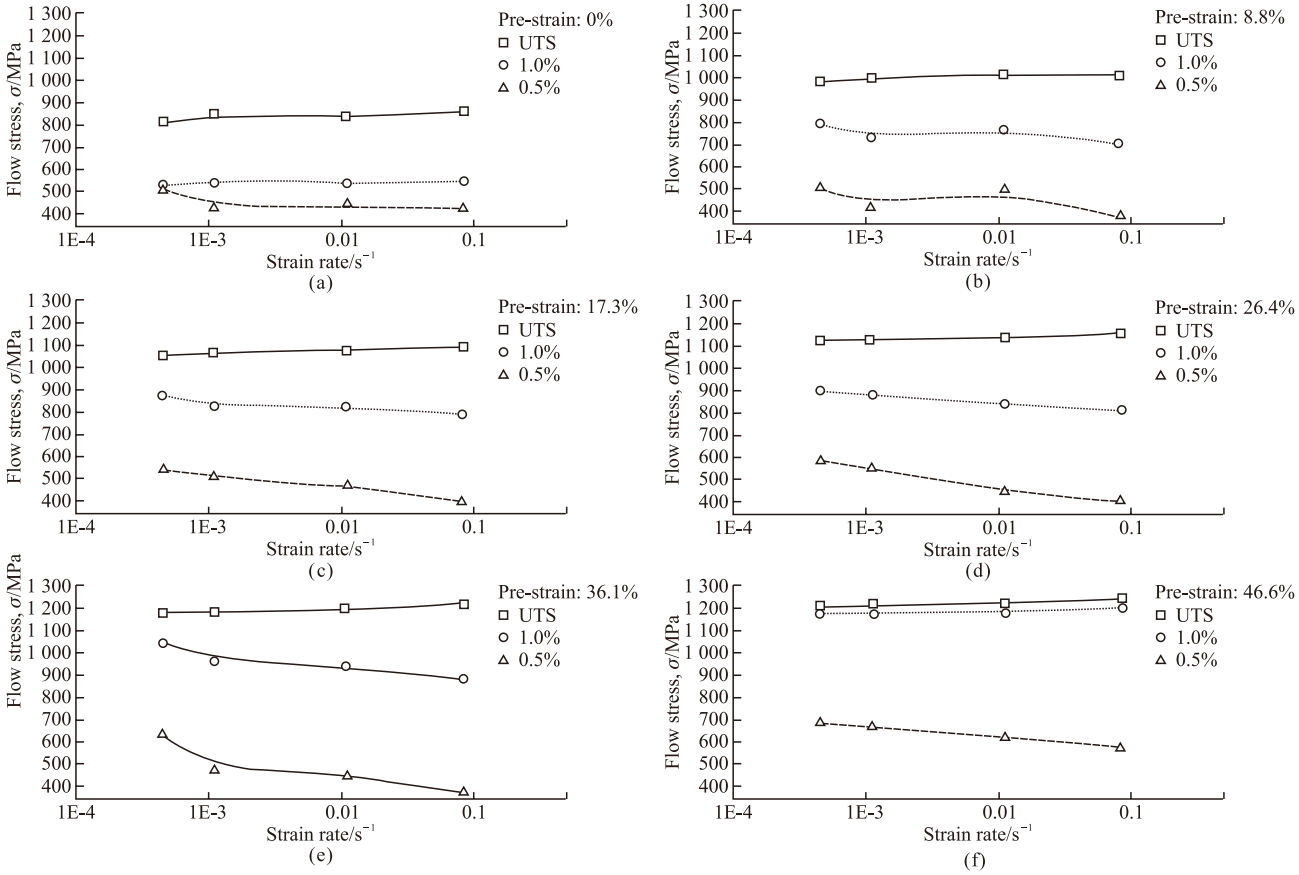

Fig.3 Flow stress versus strain rate for pre-strains Ni20Cr microwires

namic simulations of mechanical deformation of ns Cu and ns Ni suggested that the grain boundary atoms are involved in plastic deformation up to 7-10 lattice parameters[24,28-29]. The material near the grain boundaries is easier to deform, and the associated deformation mechanisms tend to be rate sensitive. Pre-strained Ni20Cr exhibited positive SRS in fracture strain, leading to increased ductility. Schwaiger studied the SRS of ns Ni at real strain rates and proposed the concept of grain-boundary affected zone[30]. This zone explains the effect of strain rate on increasing ductility. By contrast, fcc Ni20Cr possessed low stacking fault energy. Forming ns sub-grains with increasing strain rate is difficult because the grain boundary of sub-grains unbalances the movement of dislocation. The need for consistent deformation decreased to accelerate the movement of dislocation, which benefits elongation enhancement.

3.2 Effect of strain rate on flow stress

Fig.3 summarizes the flow stress versus strain rate for pre-strained Ni20Cr microwires at strain rates from 4.8×10^{-4} s^{-1} to 0.83×10^{-1} s^{-1}. Overall, the flow stresses with 0.5% plastic strain ($\sigma_{0.5\%}$) and 1% plastic strain ($\sigma_{1.0\%}$) decrease at higher strain rates, except for the $\sigma_{1.0\%}$ of pre-strain specimen with 46.4% strain. The $\Delta\sigma$ is defined as:

$$\Delta\sigma_{1.0\%}=\sigma_{1.0\%.\text{high strain rate}}-\sigma_{1.0\%.\text{low strain rate}}$$

With increasing pre-strain, the value of $\Delta\sigma_{0.5\%}$ is in the range of −85 MPa to −161 MPa, and the $\Delta\sigma_{1.0\%}$ in the range of −89 MPa to −252 MPa. That is to say the flow stresses (with 0.5% and 1.0% plastic strain) of pre-strain Ni20Cr samples decrease with an increase of the strain rate. When the pre-strain increase, this phenomenon is more obvious.

The effect of strain rate is similar to the result reported by Lu[24]. Lu has investigated the strain rate effect on the tensile behavior in ns copper. According to Fig.1 of the literature, the values of $\sigma_{1.0\%}$ and $\sigma_{0.5\%}$ decreased with an increase of the strain rate at the quasi-static condition (6×10^{-5} s^{-1} to 6×10^{-2} s^{-1}). In which, the value of $\sigma_{1.0\%}$ is about −38 MPa (decreased from 122 MPa to 84 MPa) with an increment of strain rate. So, the flow stress of the pre-strain Ni20Cr specimen exhibits the dependence on strain rate under the quasi-static condition.

According to the deformation theory and dislocation dynamics, the relationship can be expressed as follows:

$$\sigma=\left(\frac{\dot{\varepsilon}}{A\rho b}\right)^{\frac{1}{m'}}=\left(\frac{1}{A\rho b}\right)^{\frac{1}{m'}}\cdot\left(\dot{\varepsilon}\right)^{\frac{1}{m'}} \quad (1)$$

where, σ is the force on the dislocation, $\dot{\varepsilon}$ is the shear strain of one dislocation slipping distance, A is a constant, ρ is the dislocation density, b is the Burger vector, and m' is the sensitivity coefficient of dislocation movement. From the formula, the flow stress behavior can be clarified reasonably. Only if m' is a negative value, flow stress will decrease with the increase of strain rate. When the material state is determined, formula (1) can be simplified as:

$$\sigma\propto\left(\dot{\varepsilon}\right)^{M} \quad (2)$$

where, M is the strain rate coefficient. So:

$$M=\frac{1}{m'} \quad (3)$$

The strain rate coefficient for the ns Cu sample is calculated by formula (1), as shown in the Ref.[24]. From the measurement data, the strain rate coefficient

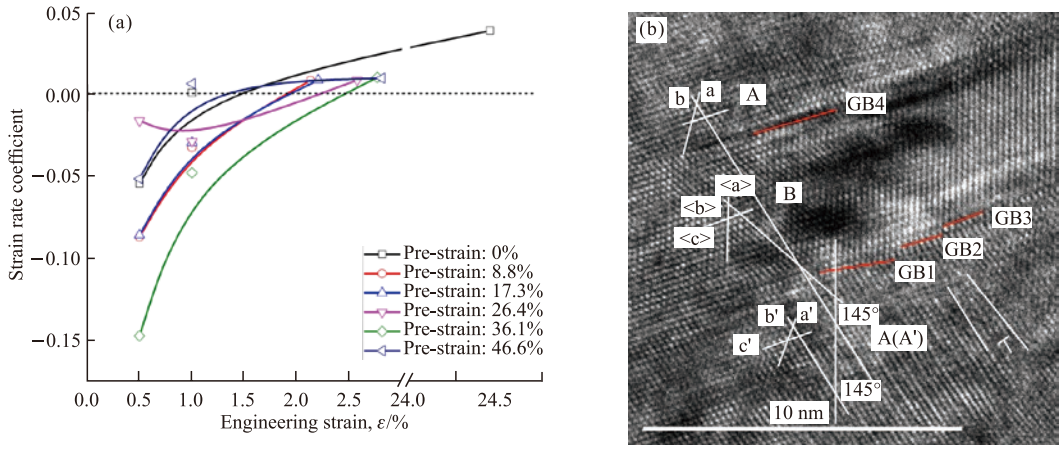

Fig.4 Variations of strain rate coefficient for pre-strains Ni20Cr microwires and deformation twin of the specimen with engineering strain 36.1% in the TD cross-section

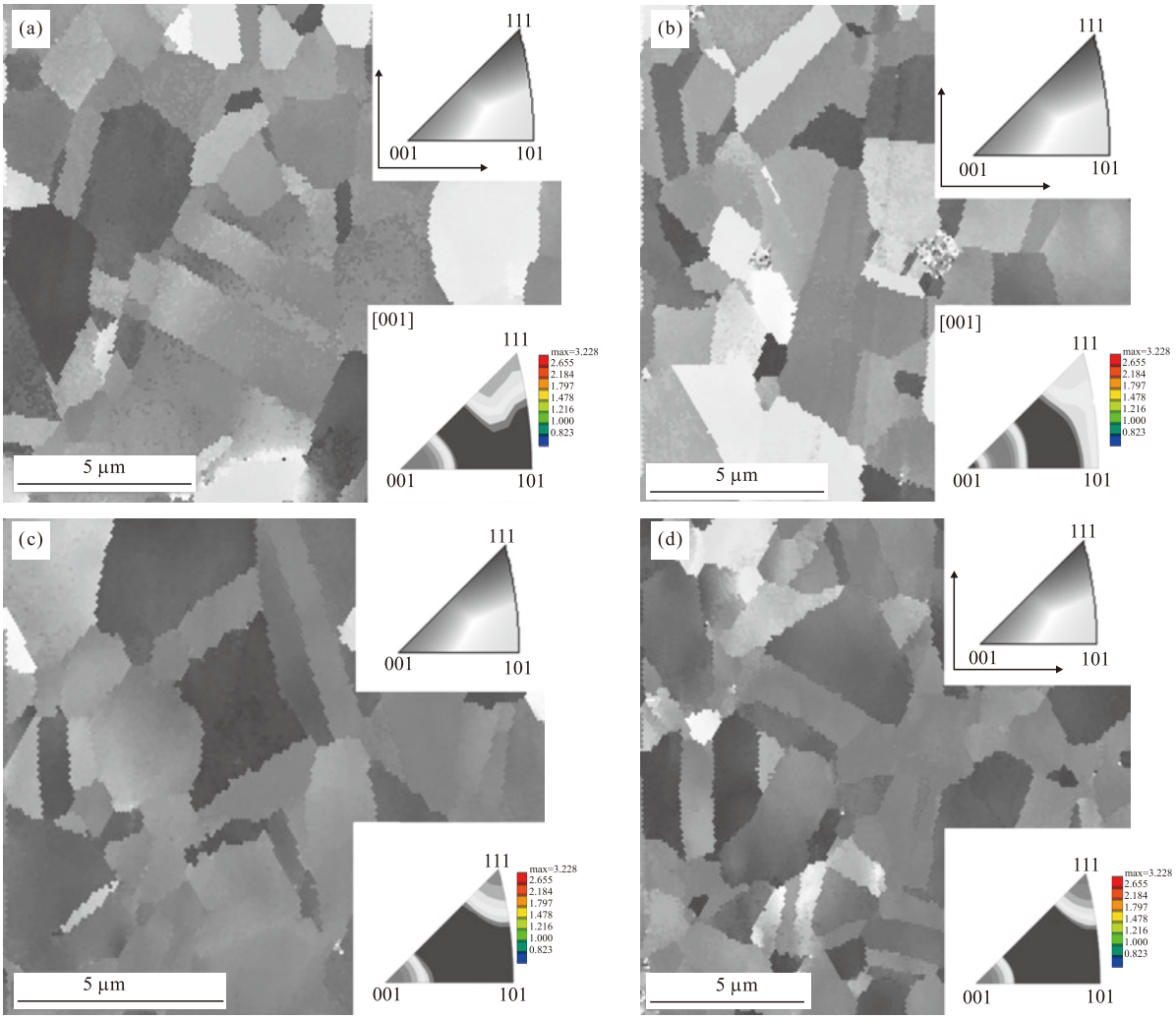

Fig.5 Grain orientations and textures of TD cross-section for different pre-strain Ni20Cr microwires: (a)0% ; (b)8.8%; (c)26.4%; (d)46.4%

for the Ni20Cr sample may be calculated by the same formula, as shown in Fig.4. The strain rate coefficient changes from negative SRS to positive SRS with increasing strain (the relative values of all specimens will be reported in another paper). When the strain exceeds a certain value, the strain rate coefficients of all pre-strain samples are positive. For example, the certain strain of pre-strain sample with 36.1% strain is about 2.5%. It is clear that fracture strain is greater than the critical strain. The UTS increases slightly with increasing strain rate. So, the fracture flow behavior of the samples did not change substantially during the tensile test at room temperature. That is to say, dislocation activities may dominate the plastic deformation of Ni20Cr near the fracture strain during the tensile tests. However, the flow behavior ($\sigma_{0.5\%}$ and $\sigma_{1.0\%}$) exhibited negative SRS, indicating that different plastic deformation mechanisms exist in initial strain zone.

Chun reported twinning-induced negative SRS in wrought Mg alloy[31]. In the research, specimens were prepared from strongly textured AZ31 plate consisted of isometric grains with an average grain size of 30 μm. Dynamic strain aging was excluded as a possible cause of negative SRS, whereas transition from negative SRS to positive SRS was considered, where twinning was saturated. Then, the alloy exhibited positive SRS at strains where slip dominated the deformation. The pre-strained Ni20Cr sample was characterized by a deformation microstructure[32], where the density of dislocations reached an extremely high level. The dislocation density in the wire cross-section (TD cross-section) with pre-strain of 46.6% was approximately 2.1×10^{16}, estimated by the high-resolution transmission electron microscopic images. Twinning deformation microstructures were noted in the TD cross-section as shown in Fig.4(b), and it was observed in the cross-section of the drawn direction (DD cross-section) in specimens with pre-strain of 36.1% and 46.6%. The accepted reason for the negative SRS at high strain rates is twinning-induced negative SRS, similar to that of wrought Mg al-

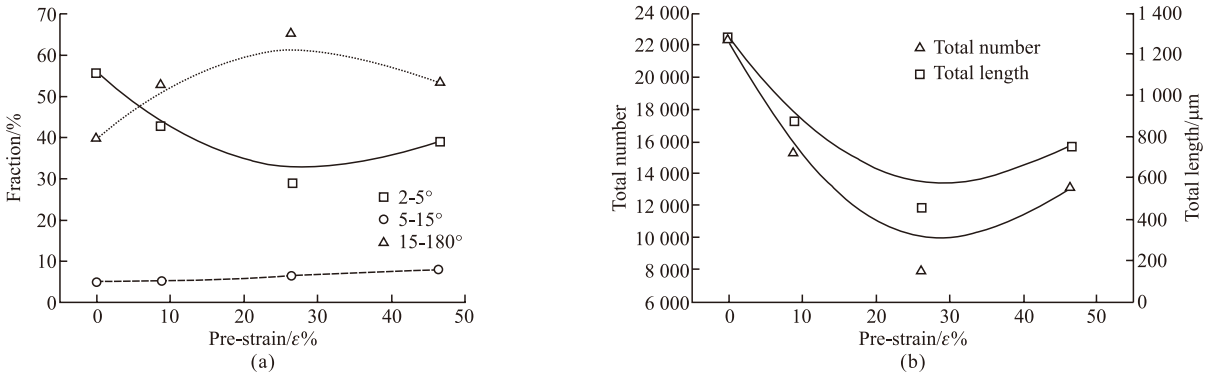

Fig.6 Fraction and length of different type grain boundaries in T. D. cross-section for different pre-strained Ni20Cr microwires

loy. Therefore, twinning deformation dominates the initial deformation stage in the pre-strain Ni20Cr tensile test. When twinning deformation reaches saturation, dislocation slip deformation dominates.

3.3 Relationship between texture and plastic deformation mechanisms

The orientation evolution of individual grain was characterized by electron backscatter diffraction analysis. Fig.5 illustrates the grain orientation and texture of TD cross-section for different pre-strained Ni20Cr microwires (upper right illustrations for the orientation, lower right illustration for [001] inverse pole figure). The relative strength color mark increased from 3.99 to 16 with increasing pre-strain. Strong textures of [001] and [111] directions, which are parallel to the drawn direction of wire, increased. Before pre-strain, a certain degree of [001] texture existed. After pre-strain, textures of [001] and [111] directions obviously increased, especially the latter.

Fig.6 demonstrates the fraction and length of different grain boundaries in TD cross-section for different pre-strained Ni20Cr microwires. From Fig.6 (a), the fraction of 5°-15° grain boundaries linearly increased with increasing pre-strain. The fraction of 15°-180° grain boundaries nonlinearly increased first and then decreased, different from 2°-5° grain boundaries. Twinning deformation produced large angle grain boundaries. Thus, changes in the fraction of 15°-180° grain boundaries induced twinning deformation. The trend confirmed that twinning deformation dominated. When twinning deformation reached saturation, dislocation slip deformation dominated. The fraction of 2°-5° and 5°-15° grain boundaries changed along with dislocation slip. The lowest fraction of 2°-5° grain boundaries appeared in a pre-strain of approximately 26.4%. Twinning deformation consumes 2°-5° grain boundaries. Upon termination of twinning deformation, the dislocation slip leads to substructure formation and lattice distortion. Consequently, the fraction of 2°-5° and 5°-15° grain boundaries increased. Moreover, 2°-5° grain boundaries induced lattice distortion, and 5°-15° grain boundaries favored substructure.

Fig.6(b) shows that the total number and length of grain boundaries nonlinearly decreased first and then increased. The lowest value appeared in pre-strain of approximately 26.4%. Afterward, internal stress increased and induced grain "fragmentation"; and the grain boundaries subsequently increased. Twinning deformation consumed 2°-5° grain boundaries, leading to a decrease in the total number and length of grain boundaries. Upon termination of twinning deformation, the dislocation slip led to substructure formation and lattice distortion. The total number and length of grain boundaries increased.

4 Conclusions

In summary, pre-strained Ni20Cr microwires exhibited positive SRS in fracture flow stress and negative SRS in flow stress $\sigma_{0.5\%}$ and $\sigma_{1.0\%}$. Fracture strain (ductility) and UTS simultaneously increased significantly at high strain rates (from 4.8×10^{-4} to 1.1×10^{-1} s^{-1}), exhibiting positive SRS. Twinning-induced negative SRS was discovered in pre-strained Ni20Cr microwires. In pre-strained Ni20Cr tensile test, twinning deformation dominated the initial deformation stage. When twinning deformation reached saturation, dislocation slip deformation dominated. The trend of the fractions of 2°-5°, 5°-15°, and 15°-180° grain boundaries confirmed the transition process.

Acknowledgements

Funded by the National Nature Science Foundation of China (No. 11135007). The authors are grateful to analyzing & measure group of General Research In-

stitute for Nonferrous Metal, GRINM, for his valuable cooperation in EBSD analysis of the specimens.

References

[1] Zhong ZW. Wire Bonding Using Insulated Wire and New Challenges in Wire Bonding[J]. *Microelectron. Int*., 2008, 25(2): 9-14

[2] Ampleford DJ, Jones B, Jennings CA, *et al*. Contrasting Physics in Wire Array Z-pinch Sources of 1-20 keV Emission on the Z Facility[J]. *Phys. Plasmas*, 2014, 21(5): 056708-1-056708-10

[3] Sinars DB, McBride RD, Pikuz SA, *et al*. Investigation of High-Temperature Bright Plasma X-ray Sources Produced in 5-MA X-Pinch Experiments[J]. *Phys. Rev. Lett*., 2012, 109(15): 155 002-1-155 002-5

[4] Ampleford DJ, Hansen SB, Jennings CA, *et al*. Opacity and Gradients in Aluminum Wire Array Z-pinch Implosions on the Z Pulsed Power Facility[J]. *Phys. Plasmas*, 2014, 21(3): 031201-1- 031201-8

[5] Gao XQ, Hu WC, Gao YS. Preparation of Ultrafine Tungsten Wire via Electrochemical Method in an Ionic Liquid[J]. *Fusion Eng. and Des*., 2013, 88: 23-27

[6] Haines MG. A Review of the Dense Z-pinch[J]. *Plasma Phys. and Control. Fusion*, 2011, 53(9): 093001(168pp)

[7] Dao M, Lu L, Asaro RJ, *et al.* Toward a Quantitative Understanding of Mechanical Behavior of Nanocrystalline Metals[J]. *Acta Mater*., 2007, 55(12): 4 041-4 065

[8] Kumar KS, Swygenhoven HV, Suresh S. Mechanical Behavior of Nanocrystalline Metals and Alloys1[J]. *Acta Mater*., 2003, 51(19): 5 743-5 774

[9] Swygenhoven HV. Grain Boundaries and Dislocations[J]. *Science*, 2002, 296(5565): 66-67

[10] Kim KS, Song JY, Chung EK, *et al*. Relationship between Mechanical Properties and Microstructure of Ultra-fine Gold Bonding Wires[J]. *Mech.Mater.*, 2006, 38(1-2): 119 -127

[11] Cho JH, Oh KH, Rollett AD, *et al*. Investigation of Recrystallization and Grain Growth of Copper and Gold Bonding Wires[J]. *Metall. Mater. Trans. A*, 2006, 37(10): 3 085-3 097

[12] He S, Houtte PV, Bael AV, *et al*. Strain Rate Effect in High-speed Wire Drawing Process[J]. *Model. Simul. Mater. Sc*, 2002, 10(3): 267-276

[13] Wei Q, Cheng S, Ramesh KT, *et al.* Effect of Nanocrystalline and Ultrafine Grain Sizes on the Strain Rate Sensitivity and Activation Volume: Fcc versus Bcc Metals[J]. *Mat. Sci Eng A-Struct.*, 2004, 381(1-2): 71-79

[14] Han BQ, Huang JY, Zhu YT, *et al*. Effect of Strain Rate on the Ductility of a Nanostructured Aluminum Alloy[J]. *Scripta Mater.*, 2006, 54(6): 1 175-1 180

[15] Wang ML, Shan AD. Effect of Strain Rate on the Tensile Behavior of Ultra-fine Grained Pure Aluminum[J]. *J. Alloy. Compd*., 2008, 455(1-2): L10-L14

[16] Zhu YT, Liao XZ. Nanostructured Metals: Retaining Ductility[J]. *Nat. Mater.*, 2004, 3(6): 351-352

[17] Gray GT. Influence of Strain Rate and Temperature on the Structure. Property Behavior of High-Purity Titanium[J]. *J. Phys. IV France*, 1997, 07(C3): 423-428

[18] Song SG, Gray GT. Influence of Temperature and Strain Rate on Slip and Twinning Behavior of Zr[J]. *Metall. Mater. Trans. A*, 1995, 26(10): 2 665-2 675

[19] Spitzig WA, Keh AS. Orientation Dependence of the Strain-rate Sensitivity and ThermallyActivated Flow in Iron Single Crystals[J]. *Acta Metall.*, 1970, 18(9): 1 021-1 033

[20] Khan AS, Liang RQ. Behaviors of Three BCC Metal over a Wide Range of Strain Rates and Temperatures: Experiments and Modeling[J]. *Int. J. Plasticity*, 1999, 15(10): 1 089-1 109

[21] Conrad H. Grain-size Dependence of the Flow Stress of Cu From Millimeters to Nanometers[J]. *Metall. Mater. Trans. A*, 2004, 35(9): 2 681-2 695

[22] Wang YM, Ma E. Strain Hardening, Strain Rate Sensitivity, and Ductility of Nanostructured Metals[J]. *Mat. Sci Eng A-Struct*., 2004, 375-377: 46-52

[23] Wang YM, Chen MW, Zhou FH, *et al*. High Tensile Ductility in a Nanostructured Metal[J]. *Nature*, 2002, 419(6910): 912-915

[24] Lu L, Li S. X, Lu K. An Abnormal Strain Rate Effect on Tensile Behavior in Nanocrystalline Copper[J]. *Scripta Mater*., 2001, 45(10): 1 163-1 169

[25] Follansbee PS, Huang JC, Gray GT. Low-temperature and High-strain-rate Deformation of Nickel and Nickel-carbon Alloys and Analysis of the Constitutive Behavior According to an Internal State Variable Model[J]. *Acta Metall. Mater.*, 1990, 38(7): 1 241-1 254

[26] Rack HJ, Cohen M. Strain Hardening of Iron-titanium Alloys at Very Large Strains[J]. *Mat. Sci Eng*., 1970, 6(5): 320-326

[27] Cheng S, Ma E, Wang YM, *et al*. Tensile Properties of in Situ Consolidated Nanocrystalline Cu[J]. *Acta Mater.*, 2005, 53(5): 1 521-1 533

[28] Schiøtz J, Vegge T, Tolla FDD, *et al*. Atomic-scale Simulations of the Mechanical Deformation of Nanocrystalline Metals[J]. *Phys. Rev. B*, 1999, 60(17): 11 971-11 983

[29] Swygenhoven HV, Spaczer M, Caro A. Microscopic Description of Plasticity in Computer Generated Metallic Nanophase Samples: a Comparison between Cu and Ni[J]. *Acta Mater.*, 1999, 47(10): 3 117-3 126

[30] Butt MZ, Sattar U. Deformation Behavior of Nickel-chromium Alloys with Special Reference to the Nature of Solute Distribution[J]. *J. Mater. Sci. Lett.*, 2001, 20(8): 759-761

[31] Chun YB, Davies CHJ. Twinning-induced Negative Strain Rate Sensitivity in Wrought Mg Alloy AZ31[J]. *Mat. Sci Eng A-Struct*., 2011, 528(18): 5 713-5 722

[32] Zhou XW, Qi YD, Liu XD, *et al.* Investigation on the Microstructure of As-deformed NiCr Microwires Using TEM[J]. *RSC Adv*., 2015, 5(110): 90 852-90 857